

Complex Systems May Not Be So Simple: Excessive Loss of Information by the Power-Law Ansatz

Sun-Ting Tsai¹, Chin-De Chang¹, Ching-Hao Chang¹, Meng-Xue Tsai¹, Nan-Jung Hsu², and Tzay-Ming Hong¹

¹*Department of Physics, National Tsing Hua University, Hsinchu 30013, Taiwan, Republic of China*

²*Institute of Statistics, National Tsing Hua University, Hsinchu 30013, Taiwan, Republic of China*

(Dated: February 5, 2019)

The ubiquity of power-law relations in empirical data displays physicists' love of simple laws and uncovering common causes among seemingly unrelated phenomena. However, many reported power laws lack statistical support and mechanistic backing, not to mention discrepancies with real data are often explained away as corrections due to finite size or other variables. We propose a simple experiment and rigorous statistical procedures to look into these issues. Making use of the fact that the occurrence frequency and pulse intensity of crumpling sound obey power law with exponent that varies with material, we simulate a complex system with two intrinsic mechanisms by crumpling two different sheets together. The probability function of crumpling sound is found to transit from two terms to a *bona fide* power law as compaction increases. This observation nicely demonstrates the effect of interactions to bring about a subtle change in macroscopic behavior, and also highlights the importance to sort the data in temporal or other order. Our analyses are based on the Akaike information criterion (AIC) that is a direct measurement of information loss and emphasizes the need to strike a balance between model simplicity and goodness of fit. As a show of force, AIC also found the Gutenberg-Richter law for earthquakes and the scale-free model for brain functional network, 2D sandpile, and solar flare intensity to suffer excessive loss of information. They resemble more the crumpled ball at low, not high, compactions; namely, there appear to be two distinct mechanisms that take turns at driving these systems.

PACS numbers: 05.40.Ca, 64.60.av, 05.65.+b

According to the classical Dulong-Petit law, the specific heat of a solid should be independent of temperature, contrary to the fact that it drops to zero at low temperature. This huge embarrassment and challenge to physicists before the nineteenth-century eventually helped hasten the birth of quantum theory. In 1907 Einstein proposed to describe each atom in the solid as an independent 3D harmonic oscillator that exhibits identical frequency and obeys Planck's quantization assumption. In spite of its historical relevance[1], this model was eventually replaced by that of Debye who linked these harmonic springs in series to generate a whole spectrum of frequencies. Both are based on the same assumption of harmonic oscillator, but Debye's more complex model turned out to explain the experimental data better.

A more contemporary puzzle concerns the abundance of simple power-law (SPL) distributions, $g(x) = \alpha/x^\beta$, over a wide range of magnitudes that surfaced in sizes of criminal charges per convict, foraging patterns of sharks and tunas, and brain activity and heart rate - to name just a few[2]. One attempt to explain their deeper origin is the concept of self-organized criticality (SOC) proposed by Bak *et al.*[3] in 1987. The power-law distribution of sand avalanches and the fact that sandpiles can come back to the critical slope without deliberate tuning of parameters have been a paradigm for SOC, although the dynamics of a real sand pile has been demonstrated[4] to behave more like a first-order transition. Another notable approach is the use of renormalization group[5], motivated by the resemblance to the power-law divergence of physical quantities with universal critical exponents in systems undergoing a smooth phase transition.

In spite of many more generative models for various reported power laws[6], statistical support and mechanistic sophistication are in dire need for improvement[2].

Crackling noise from candy wrappers and food bags is something we all hate in the cinema. A silver lining is that its occurrence rate versus pulse intensity was also reported[7] to obey SPL and may have bearing[8] on the Gutenberg-Richter law[9] for earthquakes. Exploiting the fact that exponent of crumpling sound varies with material, we simulated complex systems with two distinct mechanisms by crumpling different sheets together[10]. The data points came out aligned tantalizingly straight in a logarithmic plot - a revealing sign of SPL. For contrast, a similar analysis was repeated with the sheets crumpled by separate hands, which result was expected to distribute diffusely and in no way resemble power law. Surprisingly, it exhibits an even smaller error, $\Delta\beta$.

In order to avoid this delusion, we need to go back and understand how $\Delta\beta$ was calculated. The magnitude of β comes from maximizing the likelihood function L , while its error $\Delta\beta$ is estimated by $(-d^2 \ln L/d\beta^2)^{-1/2}$. Plug Eq.(A1) into the formula gives

$$\Delta\beta \sim \sqrt{\frac{2\sigma^2}{N \frac{d^2\sigma^2}{d\beta^2}}} \quad (1)$$

where σ denotes the standard deviation. Now imagine two independent sets of SPL data, $y_i = 1/x_i^{\beta_1} + \Delta y_i$ and $z_i = 1/x_i^{\beta_2} + \Delta z_i$ where $\beta_1 \neq \beta_2$ and $i = 1, \dots, N$ labels the slices in the histogram. For simplicity, let's suppose the random numbers Δy_i and Δz_i render relatively small

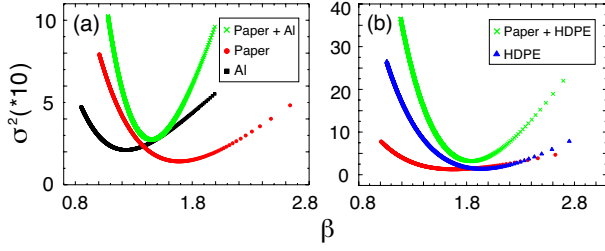


FIG. 1: Standard deviation plotted against fitting exponent of SPL for crumpling sound. $(\Delta\beta)^2$ is proportional to the ratio of $\sigma^2(\beta)$ and its curvature. (a) Paper (in red circle) and Al (in black square) and their combined data (in green cross). The optimal β can be read off from the minima position to be 1.68, 1.22, and 1.44. Combined data exhibit a large curvature, which results in a misleadingly small $\Delta\beta = 0.0126$, compared to 0.0198 and 0.0200 for paper and Al. (b) Paper and HDPE (in blue triangle, $\beta = 1.94$, $\Delta\beta = 0.0143$) and their combined data ($\beta = 1.84$, $\Delta\beta = 0.0128$).

$\Delta\beta_k/\beta_k$ for $k = 1, 2$. According to Eq.(1),

$$(\Delta\beta_k)^2 \sim \frac{1}{N} \frac{\sum_{i=1}^N (\Delta y_i)^2}{\sum_{i=1}^N x_i^{-2\beta_k} (\ln x_i)^2}, \quad k = 1, 2 \quad (2)$$

where a statistical average over the random numbers is implied. If both data are combined and fit by SPL out of ignorance, Eq.(1) gives

$$(\Delta\beta)^2 \sim \frac{\sum_i [(\alpha x_i^{-\beta} - x_i^{-\beta_1} - x_i^{-\beta_2})^2 + (\Delta y_i)^2 + (\Delta z_i)^2]}{N \sum_i (x_i^{-2\beta_1} + x_i^{-2\beta_2} + 2x_i^{-\beta_1 - \beta_2}) (\ln x_i)^2}, \quad (3)$$

under a general scenario[10].

In the case of perfect power laws, i.e., $\Delta y_i = \Delta z_i = 0$ and $\Delta\beta_{1,2} = 0$, Eq.(3) predicts $\Delta\beta > \Delta\beta_i, \forall i = 1, 2$, as expected for our rash move. However, as long as $\Delta\beta_i \neq 0$ and exceeds about 2×10^{-4} , the ratio of first terms in the numerator and the denominator of Eq.(3) becomes smaller than the subsequent ratio of second and third terms. A closer look reveals that the second and third ratios are simply $\Delta\beta_1$ and $\Delta\beta_2$ from Eq.(2). It takes only simple arithmetic to be convinced that $\Delta\beta < \max\{\Delta\beta_1, \Delta\beta_2\}$. The reasoning behind this counterintuitive result is due to the misuse of Eq.(1) for $(\Delta\beta)^2$ when the fitted model is wrong, i.e., SPL model is fitted to DPL data in our case. For this model misspecification situation, a correction for $(\Delta\beta)^2$ should be adopted using Huber's sandwich estimation[11], while applied users are seldom aware of this issue.

Figure 1 shows $\sigma^2(\beta)$ for Al, paper, and HDPE and the combination of their data - all modeled by SPL. The much larger curvature for the combined data results in a smaller $\Delta\beta$ according to Eq.(1) in spite of a large σ . Due to their β being distinct, the correct fitting function is double power-law (DPL), $\alpha_1/x^{\beta_1} + \alpha_2/x^{\beta_2}$, rather than SPL. However, since increasing fitting parameter almost always improve the standard deviation, we cannot rely

on the likelihood function alone to measure their relative fitting performance. It is thus imperative to seek other information criterion that also takes into account the principle of parsimony or model simplicity.

Founded on information theory, the Akaike information criterion[12] (AIC) came to our rescue. It quantifies the relative fitting performance of distribution functions, $g(x)$, for a given set of data. As described by the Kullback–Leibler (KL) distance[13] which measures the information loss when using $g(x)$ to approximate the true distribution, AIC value is defined as

$$\text{AIC} = 2k - 2 \ln L \quad (4)$$

where the first term penalizes the abuse of free parameters, k , and the likelihood function L rewards goodness of fit. Smaller AIC value indicates less information loss. This trade-off between goodness of fit and model simplicity bears resemblance to the Helmholtz free energy, $F \equiv U - TS$ where T denotes the temperature, for canonical ensembles in equilibrium statistical mechanics. In contrast to Eq.(4), F balances the competing trends of minimizing internal energy U and maximizing entropy S .

The likelihood function is defined as

$$L \equiv \prod_{i=1}^n g(x_i) \quad (5)$$

where n is the number of raw data and $g(x)$ the fitting functions. After the data has been grouped into a histogram of N slices, the log-likelihood function becomes

$$\ln L \equiv n \sum_{j=1}^N f(x_j) \ln g(x_j), \quad (6)$$

where $n f(x_j)$ denotes the counts of j -th slice. Since both $f(x)$ and $g(x)$ are destined to describe probability density functions, it is important to remember to impose the normalization: $\sum f(x_i) = \int g(x) dx = 1$.

The schematic Fig.2 illustrates the relationship between DPL and the Zipf-Mandelbrot distribution[14] (ZMD), $g(x) = \alpha/(x + \gamma)^\beta$, and other functions[15] that are often checked against SPL. ZMD and DPL are generalized versions of SPL and unlike the log-normal (LN), exponential (EX), and Poisson (PS) distributions that are the simplest form in their own category. However, being closer to the data in Fig.2, DPL and ZMD enjoy less information loss, although more complex than SPL.

Armed with the AIC tool, we did a more thorough analysis on the jointly crumpled data by separating them into five time stages in Fig.3. A transition from DPL to SPL was revealed as compaction increases, which confirms the prediction by Gleeson *et al.*[16] that interactions can bring out a subtle change in macroscopic behavior. Note that the initial data can be easily passed for power law, if not for the scrutiny of AIC. Since the exponents of DPL determined by the likelihood function match the singly crumpled data, the second power law

TABLE I: Comparing AIC values of different models for celebrated power-law claims. The parameters of selected model are highlighted in boldface. The magnitudes of $\alpha_{1,2}$ are comparable, but only their signs are included for brevity.

Phenomenon	SPL		DPL			ZMD	
	AIC	β	AIC	(α_1, α_2)	(β_1, β_2)	AIC	(γ, β)
Earthquake[18]	133115.7	1.03	133112.9	(+,+)	1.10, 0.76	133117.7	-0.01, 1.03
Brain Functional Network[19]	11456.73	2.33	11420.49	(+,+)	3.42, 1.62	11422.94	-3.33, 1.82
Solar Flare Intensity[6]	72028.82	2.10	71431.24	(+,+)	3.76, 1.75	71439.20	-37.07, 1.74
2-D Sandpile Model[20]	1266784	1.01	1266651	(-,+)	0.77, 0.91	1266656	0.17, 1.04
Solar Flare Rate[21]	54747.96	1.10	54561.22	(+,-)	0.87, 0.77	54201.22	48.08, 2.10
Web Link[22]	1095357310	1.72	1094847304	(+,+)	1.46, 1.71	1087235440	0.75, 2.03
Protein-Domain Frequency[14]	17445.29	0.56	17427.53	(+,-)	0.85, 0.94	17422.58	3.89, 0.81
Stock-Market Fluctuation[23]	18275.57	3.25	18258.62	(-,+)	2.43, 3.02	18200.94	1.70, 5.82

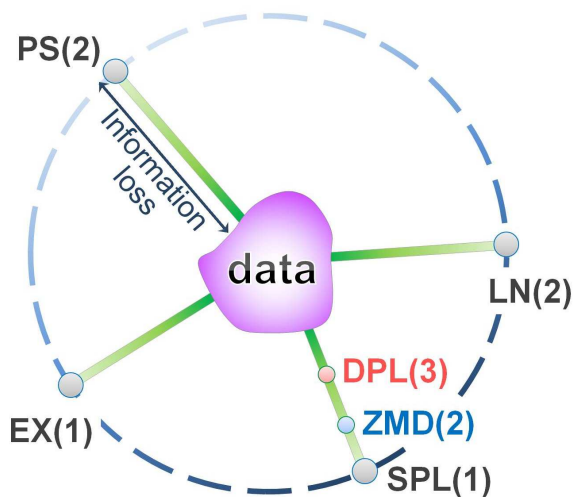


FIG. 2: Schematic relation of information loss by different models. Number of free parameters is indicated in the parenthesis following each distribution. Distance between each point and the data in this model space reflects the amount of information loss as measured by the KL distance. The dash line traces out a set of distributions with their simplest form. In contrast, DPL and ZMD are on the same green solid line as SPL since they belong to the same category.

cannot be dismissed as correction to SPL due to some relevant variable[17].

In Table I, we highlighted more power-law claims that suffer excessive loss of information. Up to ten terms have been checked not to be the winner, except in the Zipf's law for word frequency[24] where quadruple power laws were found to retain the most information. AIC concludes that DPL should replace SPL in earthquake[25], brain functional network, solar flare intensity, and 2D sandpile model (poster boy of SOC). As Fig.4 shows, DPL and SPL are hard to discern by bare eyes. For the data in Fig.4(a) that span 33 years until 2013, the Gutenberg-Richter law predicts a probability of 0.000260 for earthquakes[18] of Richter scale 6 to 8 to occur. But according to DPL parameters in Table I, the forecast

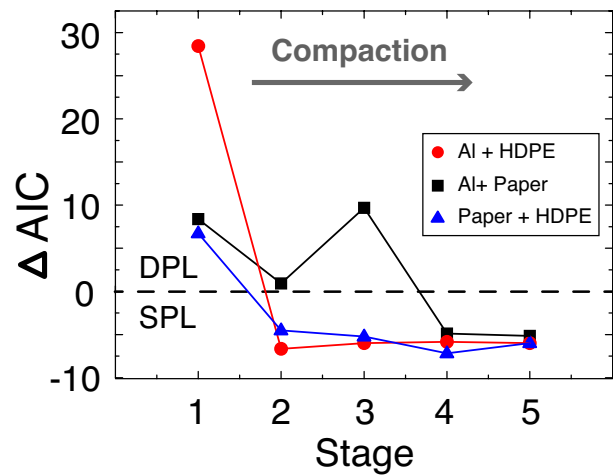


FIG. 3: AIC analyses of sound for two materials crumpled together. Data were divided into five time stages with 1 being the earliest. The y -axis showed the difference of AIC value between DPL and SPL. As compaction increases, the crumpled ball exhibits a subtle transition from DPL to SPL.

moves up by almost two folds to 0.000464. This discrepancy is statistically significant to warrant attentions. Table I also reported ZMD to be more favored for the duration-time frequency of solar flare, web link, protein-domain frequency, and stock-market fluctuations.

The quantities listed in Table I all exhibit a large difference in AIC values. This guarantees the likelihood ratio rejects SPL as a null hypothesis and preserves the more general form of DPL and ZMD. In other words, although SPL is protected as the existing model, the stricter likelihood ratio test makes sure that the evidence is strong enough to dismiss it as long as the following condition is met when the sample size is large[26]:

$$-2 \ln \frac{L_1}{L_2} > \chi_{0.95}^2(k_2 - 1) \quad (7)$$

where L_1 is the likelihood function for SPL and $\chi_{0.95}^2(k_2 - 1)$ equals 5.99 (3.84) when L_2 represents DPL (ZMD) which corresponds to $k_2 = 3$ (2). The condition, Eq.(7),

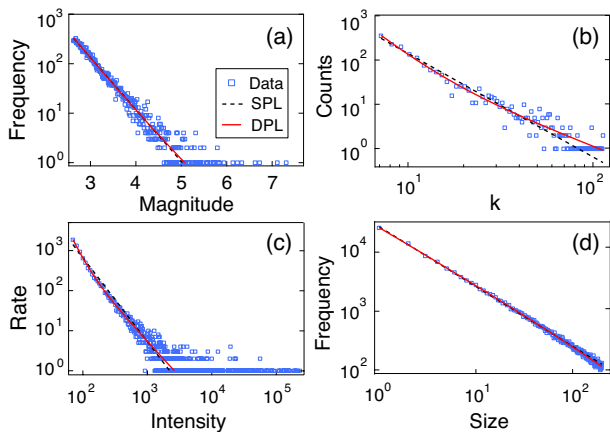


FIG. 4: Notable power law claims that require modifications. The DPL (in red solid line) outperforms SPL (in black dash line) for (a) earthquakes[18], (b) brain functional network[19], and (c) solar flare intensity[6], and (d) 2D sandpile model[20].

can be equivalently verified via

$$\text{AIC}_1 - \text{AIC}_2 > \chi_{0.95}^2(k_2 - 1) - 2(k_2 - 1) \quad (8)$$

which clearly holds for all cases in Table I.

In conclusion, by bridging the gap with mathematicians we introduced the Akaike information criterion to quell the criticism that many reported power laws lack statistical support. It turned out that there are alternative models that retains more information than power law in many famous phenomena. We found them to behave like a loosely crumpled ball consisting of two different materials - in the sense that two distinct mechanisms take turns at appearing. By analyzing the crumpling sound in temporal order, more features surfaced: it transits from DPL to SPL as compaction increases. This observation confirms the generally accepted prediction that interactions can bring about a subtle change in macroscopic behavior, and also highlights the possibility of retrieving more information if efforts are made to sort the data in either temporal or other order.

We have to admit that we do not understand why there are so few examples of thrice or higher power laws in our study, why the 2-D sandpile model should betray its role as a paradigm for SOC by behaving like DPL, or what is the physical implication for DPL exhibiting negative α .

Derived from the Kullback-Leibler discrepancy, AIC provides a simple and effective way to select the best approximation model among competitors. With the optimal property of being asymptotic efficiency, it outperforms other selection criteria, such as BIC, for selecting predictive models[27]. Due to its being based on information theory, AIC is relevant to the Landauer's principle[28] and recent interest in using entropy transfer[29] to quantify directed statistical coherence between spatiotemporal processes. It can be said that AIC is essentially an application of the Second Law of Thermodynamics[12, 30], while Landauer's principle is a

simple logical consequence of the law. Although AIC is originally intended for probability density functions, we describe in Appendix how to generalize it to tackle dimensional data, such as pressure versus volume for gases.

We acknowledge funding from the Ministry of Science and Technology and hospitalities of the Physics Division of National Center for Theoretical Sciences in Hsinchu. We also thank Hsuan-Yi Chen, Chun-Chung Chen, Jim Sethna, and Mason A. Porter for helpful comments.

Appendix A: How to use AIC without information of raw data?

It is always preferable to work with the raw data. However, if they are not available or when the data refer to (pressure, volume) of a gas or (pressure, mass density) of a crumpled ball, Eq.(6) cannot be used. Reasons are simple: no information of n for one thing, it is meaningless to compare $\ln L$ with $2k$ in Eq.(4) because Eq.(6) now carries units. Instead, we appeal to Eq.(5) for AIC.

First, suppose we know a priori that the data (x_i, y_i) are close to the set $(x_i, m_\theta(x_i))$ with small errors, where $m_\theta(x_i)$ contains unknown parameters, $\theta = (\theta_1, \theta_2, \dots)$. We then assume the errors, $\varepsilon_i = y_i - m_\theta(x_i)$, obey the normal distribution and use the Gaussian likelihood in Eq.(5). The normal assumption often holds for experimental data, in particular when data come from grouping or averaging due to central limit theorem. Under this fairly general assumption, Eq.(5) becomes

$$L = \prod_{i=1}^N \frac{1}{\sqrt{2\pi\sigma^2}} \exp\left(-\frac{(y_i - m_\theta(x_i))^2}{2\sigma^2}\right). \quad (\text{A1})$$

By setting $dL/d\sigma = 0$, it is straightforward to show that the variant that maximizes the likelihood is nothing but the mean squared errors:

$$\sigma^2 \equiv (1/N) \sum_{i=1}^N (y_i - m_\theta(x_i))^2, \quad (\text{A2})$$

subject to θ . By using this information and taking logarithm, Eq.(A1) reduces to $-(N/2) \ln(\sigma^2) - N/2$. The constant term $N/2$ is irrelevant when comparing different AIC values. Then AIC has a succinct form

$$\text{AIC} = 2k + N \ln(\hat{\sigma}^2) \quad (\text{A3})$$

where $\hat{\sigma}^2$ is the minimizer of Eq.(A2) which turns out to be equivalent to the familiar method of least square in a regression.

If the data are accompanied with known error bars σ_i , the likelihood function in Eq.(A1) should be modified as

$$L = \prod_{i=1}^N \frac{1}{\sqrt{2\pi\sigma_i^2}} \exp\left(-\frac{(y_i - m_\theta(x_i))^2}{2\sigma_i^2}\right) \quad (\text{A4})$$

with the width of the Gaussian function input from experimental observations. Taking logarithm now leads to

the form $\ln L = C - (1/2) \sum (y_i - m_\theta(x_i))^2 / \sigma_i^2$ where constant C is again not important and maximizing the second term is equivalent to minimizing the weighted least squares:

$$\chi^2 \equiv \sum_{i=1}^N (y_i - m_\theta(x_i))^2 / \sigma_i^2, \quad (\text{A5})$$

subject to θ . AIC value becomes

$$\text{AIC} = 2k + \chi^2. \quad (\text{A6})$$

As a close connection, the minimizer of Eq.(A5) can also

be used to perform a χ^2 goodness-of-fit test.

For the scenarios this appendix is aimed for, the raw data either have been gathered into histogram or carry units. As a result, the sample size is normally limited, i.e., the bin size N might not be much larger than k . In these cases AIC tends to pick an over-fit model and needs a bias-correction[30, 31] by AICc:

$$\text{AICc} = \text{AIC} + \frac{2k(k+1)}{N-k-1} \quad (\text{A7})$$

with the correction term that goes to zero when $N \gg k$.

-
- [1] R. Eisberg and R. Resnick, *Quantum Physics of Atoms, Molecules, Solids, Nuclei, and Particles* (John Wiley & Sons, 1985) 2nd ed..
- [2] More examples can be found in M. P. H. Stumpf and M. A. Porter, *Science* **335**, 665 (2012) and Ref.[6].
- [3] P. Bak, C. Tang, and K. Wiesenfeld, *Phys. Rev. Lett.* **59**, 381 (1987); C. Tang and P. Bak, *Phys. Rev. Lett.* **60**, 2347 (1988).
- [4] H. M. Jaeger, C. H. Liu, and S. R. Nagel, *Phys. Rev. Lett.* **62**, 40 (1989); S. R. Nagel, *Rev. Mod. Phys.* **64**, 321 (1992).
- [5] J. P. Sethna, K. A. Dahmen, and C. R. Myers, *Nature (London)* **410**, 242 (2001).
- [6] M. E. J. Newman, *Contemporary Physics* **46**, 323 (2005).
- [7] E. M. Kramer and A. E. Lobkovsky, *Phys. Rev. E* **53**, 1465 (1996); P. A. Houle and J. P. Sethna, *Phys. Rev. E* **54**, 278 (1996).
- [8] R. S. Mendes *et al.*, *Euro. Phys. Lett.* **92**, 29001 (2010).
- [9] B. Gutenberg and C. F. Richter, *Bull. Seismol. Soc. Amer.* **34**, 185 (1944).
- [10] See Supplemental Material for more details.
- [11] P. J. Huber, *Proceedings of the Fifth Berkeley Symposium on Mathematical Statistics and Probability*, vol. I, pp. 22-33 (1967).
- [12] H. Akaike, *Proceedings of the 2nd International Symposium on Information Theory*, edited by B. N. Petrov and F. Csaki (Armenia, USSR, 1971), 267-281; *IEEE Transactions on Automatic Control* **19**, 6, 716 (1974); *A Celebration of Statistics*, edited by A. C. Atkinson and S. E. Fienberg (Springer, 1985), 1-24.
- [13] J. deLeeuw, *Breakthroughs in Statistics, Volume I*, edited by S. Kotz and N. L. Johnson (Springer, 1992), 599-609.
- [14] The original Zipf-Mandelbrot distribution was destined for discrete data and ranked distribution, such as word frequency and aftershock activity. G. K. Zipf, *Human Behavior and the Principle of Least Effort* (Addison-Wesley, Boston, 1949); B. Mandelbrot, *The Fractal Geometry of Nature* (Freeman, San Francisco, 1983); and T. Utsu, Y. Ogata, and R. S. Matsu'ura, *J. Phys. Earth* **43**, 1 (1995).
- [15] A. Clauset, C. R. Shalizi, and M. E. J. Newman, *SIAM Review* **51**, 661 (2009).
- [16] J. P. Greason, D. Cellai, J.-P. Onnela, M. A. Porter, and F. Reed-Tsochas, *PNAS* **111**, 10411 (2014).
- [17] J. P. Sethna (private communication).
- [18] These data were collected from the SCSN Focal Mechanism Catalog and spanned the period from 1981 to 2013. <http://scedc.caltech.edu/research-tools/alt-2011-yang-hauksson-shear>
- [19] V. M. Eguiluz, D. R. Chialvo, G. A. Cecchi, M. Baliki, and A. V. Apkarian, *Phys. Rev. Lett.* **94**, 018102 (2005); B. J. He, *Trends in Cognitive Sciences*, **18**, 480 (2014).
- [20] <http://www.phy.duke.edu/~palmer/notebooks/csindex.html> is acknowledged for the source code.
- [21] F. Y. Wang and Z. G. Dai, *Nature Phys.* **9**, 465-467 (2013).
- [22] A. Broder, R. Kumar, F. Maghoul, P. Raghavane, S. Rajagopalan, R. Stata, A. Tomkins, and J. Wiener, *Computer Networks* **33**, 309 (2000).
- [23] X. Gabaix, P. Gopikrishnan, V. Pleaou and H. E. Stanley, *Nature* **423**, 267 (2003); *MIT Department of Economics Working Paper No. 03-30* (2005). We followed these two papers at defining normalized stock-price return, and analyzed the daily close price of NYSE from December 31, 1965 to May 3, 2015. Data were downloaded from <http://finance.yahoo.com/q/hp?s=^NYA+Historical+Prices>. We checked that the cumulative plot and magnitude of power-law exponent (if fitted by SPL) were similar to those on pages 46 and 47 of the latter work.
- [24] Based on the novel, *Moby Dick*, by Hermann Melville.
- [25] D. Schorlemmer, S. Wiemer, and M. Wyss, *Nature* **437**, 539 (2005) concluded that the exponent of Gutenberg-Richter law could vary for different styles of faulting. However, our data were collected without screening to retain particular rake angles.
- [26] S. S. Wilks, *The Annals of Mathematical Statistics* **9**, 60 (1938).
- [27] K. P. Burnham and D. R. Anderson, *Sociological Methods & Research* **33**, 261 (2004); K. Aho, D. Derryberry, T. Peterson, *Ecology* **95**, 631 (2014).
- [28] R. Landauer, *IBM Journal of Research and Development* **5**, 183-191 (1961); A. Berut, A. Arakelyan, A. Petrosyan, S. Ciliberto, R. Dillenschneider, and E. Lutz, *Nature* **483**, 187 (2012).
- [29] M. Prokopenko and J. T. Lizier, *Scientific Reports* **4**, 5394 (2014).
- [30] K. P. Burnham and D. R. Anderson, "Model Selection and Multimodel Inference: A Practical Information - Theoretic Approach" (Springer-Verlag, 2002) 2nd ed.
- [31] C. M. Hurvich and C. L. Tsai, *Biometrika* **76**, 297-307 (1989).